Journal of Computational Physics 258 (2014) 1–14

Contents lists available at ScienceDirect

Journal of Computational Physics

www.elsevier.com/locate/jcp

A fast numerical method for computing doubly-periodic regularized Stokes flow in 3D

Ricardo Cortez, Franz Hoffmann *

Department of Mathematics, Tulane University, New Orleans, LA 70118, USA

ARTICLE INFO

Article history:
Received 10 March 2013
Received in revised form 11 October 2013
Accepted 17 October 2013
Available online 23 October 2013

Keywords:
Stokes flow
Ewald summation
FFT

ABSTRACT

A new numerical method for computing three-dimensional Stokes flow driven by a doubly-periodic array of regularized forces is presented. The method is based on deriving an analytical representation of a regularized Green's function in Fourier space. Then only an inverse fast Fourier transform (inverse FFT) has to be computed to determine the fluid velocity on a grid in the physical domain. The velocity at other points can be interpolated from this grid. Accuracy is verified by comparing numerical results to a solution that is independent of the method. Although the regularized forces lead to a smooth velocity field, the Green's function may contain rapid transitions that are not captured properly on a coarse grid. In that case, an Ewald splitting technique is used to compute the grid-resolved part of the flow using an inverse FFT and a sum in physical space for the localized part of the velocity. The splitting parameter can be chosen as small as a few grid cells, which makes the sum in physical space converge extremely fast. We present numerical examples that demonstrate that fact. In some cases, when the grid size is sufficiently small compared to the regularization parameter, the Ewald splitting is not needed.

1. Introduction

We present a numerical method for computing doubly periodic Stokes flow in three dimensions. Stokes flow is relevant when viscous forces dominate inertial forces, as is the case in highly viscous fluids or when the length scales in the problem are tiny. We are motivated by periodic flows created, for instance, by synchronized beating of cilia [1]. Cilia are hair-like structures found on the surfaces of cells and their arrangement on a two-dimensional surface makes the flow doubly-periodic. Coordinated beating of cilia plays a role in the transport of fluids or the locomotion of microorganisms. In this paper we will focus our attention on numerical aspects.

Consider first incompressible Stokes flow driven by N singular forces in unbounded three-dimensional space without periodicity. The Stokes equations are

$$\begin{aligned} 0 &= \mu\Delta\mathbf{u} - \nabla p + \sum_{n=1}^{N} \mathbf{f}_n \delta(\mathbf{x} - \mathbf{x}_n), \\ 0 &= \nabla \cdot \mathbf{u}, \end{aligned} \tag{1}$$

where $\mathbf{u}$ is the fluid velocity, p is pressure and μ is the fluid viscosity. The external force is a linear combination of Dirac delta distributions. The second equation is the incompressibility condition. The solution is a sum of *Stokeslets* given by

* Corresponding author. Tel.: +1 504 862 8391.
E-mail addresses: rcortez@tulane.edu (R. Cortez), fhoffma@tulane.edu (F. Hoffmann).

0021-9991/$ – see front matter
http://dx.doi.org/10.1016/j.jcp.2013.10.032

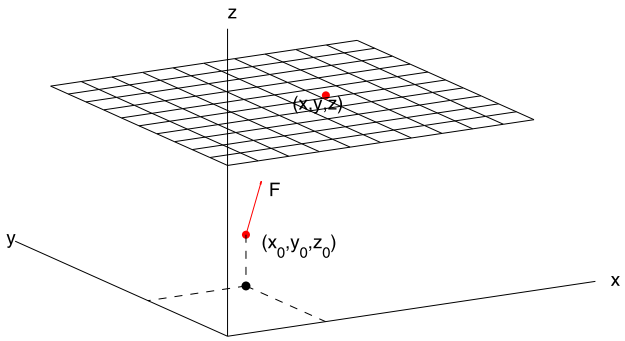

Fig. 1. Schematic for the computation of the velocity field at a point (x, y, z).

$$\mu \mathbf{u}(\mathbf{x}) = \sum_{n=1}^{N} \frac{\mathbf{f}_n}{8\pi |\mathbf{x}-\mathbf{x}_n|} + \frac{[\mathbf{f}_n \cdot (\mathbf{x}-\mathbf{x}_n)](\mathbf{x}-\mathbf{x}_n)}{8\pi |\mathbf{x}-\mathbf{x}_n|^3}. \tag{2}$$

We note that the fluid velocity in Eq. (2) is singular at the locations $\mathbf{x} = \mathbf{x}_n$ as a result of the force delta distribution. This velocity can also be written as

$$\mu \mathbf{u}(\mathbf{x}) = \sum_{n=1}^{N} \big((\mathbf{f}_n \cdot \nabla)\nabla - \mathbf{f}_n \Delta \big) B(r_n), \tag{3}$$

where $r_n = |\mathbf{x}-\mathbf{x}_n|$ and the Green's function $B(r) = -r/8\pi$ is the fundamental solution to the biharmonic operator Δ^2, i.e.

$$\begin{aligned} \Delta G(r) &= \delta(r), \\ \Delta B(r) &= G(r), \end{aligned} \tag{4}$$

where $G(r) = -1/8\pi r$.

Turning now to solving this problem in a doubly-periodic domain, we consider point forces $\mathbf{f}_n$ that lie in the *main domain* $[0, L] \times [0, L] \times \mathbb{R}$ and are distributed periodically in x and y with period L. In order to compute the velocity corresponding to the doubly-periodic array of forces, we can consider the velocity contributions of all forces and of their periodic copies. This yields an infinite double-sum for each of the forces in the main domain. In the case of zero net force, $\sum_{n=1}^{N} \mathbf{f}_n = \mathbf{0}$, the infinite double sums converge but slowly and the velocity singularities remain. A standard approach to evaluate efficiently the infinite series is to employ an Ewald splitting [2], where the series is split into a smooth part that can be computed efficiently in Fourier space and a fast-decaying local part (containing the singularity) to be computed in physical space. This approach is not straight forward for doubly-periodic domains in three dimensions, as explained in [2].

Our goal is to develop a general method that can be applied to problems with doubly-periodic flows in three dimensions for any given configuration of forces. To remove the singularity from the solution, we use a regularized force field obtained by replacing the delta functions in Eq. (1) with a narrow Gaussian function $\Phi_\varepsilon(r)$, where ε is a numerical parameter that controls the width of the function. The analytic solution of Eq. (1) with regularized forces is known as a *regularized Stokeslet* and it approximates the singular Stokeslet away from the singularities while remaining smooth throughout the domain [3].

Besides using regularized forces, the method presented here differs from the standard Ewald splitting technique in the way the smooth part of the flow is computed. Instead of approximating an infinite sum in spectral space, we derive analytic expressions for the Green's function in Fourier space (corresponding to the variables x and y only). In other words, we find an expression for the Fourier space version of the regularized Green's function, $\hat{B}_{\Phi_\varepsilon}(k, m, z)$, where k and m are the wave numbers corresponding to x and y, respectively. Given the exact expression for $\hat{B}_{\Phi_\varepsilon}(k, m, z)$, the Fourier space form of the velocity field is easily found from the Fourier space form of Eq. (3). In order to compute the fluid velocity in the physical domain, we fix a value of z and create a two-dimensional grid of wave numbers (k, m), each from 0 to a maximum integer, where we evaluate the transform of the velocity. We then use an inverse fast Fourier transform (inverse FFT) to get the fluid velocity on an (x, y) grid at the fixed value of z. Fig. 1 shows a schematic of this set up.

It might seem unnecessary to use an Ewald splitting in the case of regularized forces since the fluid velocity is smooth in this case. The smoothness of the velocity should translate into fast-decaying Fourier coefficients without needing to isolate a non-smooth local term to be computed in physical space. However, in the method of regularized Stokeslets [3], the function $\Phi_\varepsilon(\mathbf{x})$ converges as a distribution to a delta function in the limit as $\varepsilon \to 0$. For this reason, in practice, the regularization parameter ε should be small. Consequently, the force $\mathbf{f}\Phi_\varepsilon(\mathbf{x})$, although smooth, is spiky. In particular, if ε is small compared to the FFT grid spacing, the regularized force is not properly resolved on the grid. As a result, taking the inverse FFT of the regularized Stokeslet leads to an oscillatory solution. For this reason we provide a way to use Ewald splitting where the traditional Fourier space sum is replaced by an FFT on the grid, which guarantees fast computation, and a local velocity

Table 1
Diagram showing the proposed method for solving Stokes equation in Fourier space driven by one point force $\mathbf{f}$ centered at the origin. The solution for a general distribution of point forces follows readily from the linearity of Stokes equation. Here, k and m are the wave numbers in the x and y directions, and the gradient and Laplace operators in Fourier space are defined by $\hat{\nabla} = (ik, im, \frac{\partial}{\partial z})$ and $\hat{\Delta} = (-k^2 - m^2 + \frac{\partial^2}{\partial z^2})$.

$$\boxed{\Delta^2 B_{\Phi_\varepsilon}(|\mathbf{x}|) = \Phi_\varepsilon(|\mathbf{x}|)}$$

Fourier transform in x and y

$$\boxed{(k^2+m^2)^2 \hat{B}_{\Phi_\varepsilon}(k,m,z) - 2(k^2+m^2)\hat{B}''_{\Phi_\varepsilon}(k,m,z) + \hat{B}''''_{\Phi_\varepsilon}(k,m,z) = \hat{\Phi}_\varepsilon(k,m,z)}$$

Solve ODEs in z

$$\boxed{\text{Green's function } \hat{B}_{\Phi_\varepsilon}(k,m,z)}$$

apply operator $\frac{1}{\mu}((\mathbf{f}\cdot\hat{\nabla})\hat{\nabla} - \mathbf{f}\hat{\Delta})$

$$\boxed{\hat{\mathbf{u}}(k,m,z)}$$

inverse FFT in k and m

$$\boxed{\mathbf{u}(\mathbf{x})}$$

computation is done in physical space. We show numerically that the splitting parameter can be chosen as small as a few multiples of the FFT grid spacing, which makes the physical space sum converge extremely fast. We also show that if the FFT grid is sufficiently fine compared to the regularization parameter ε, there is no need for the Ewald splitting and the entire process can be done as described in this section and depicted in Table 1.

The rest of the paper is organized as follows. In Section 2 we derive all formulas for the doubly periodic regularized Stokeslet in Fourier space. In Section 3 we detail how the Ewald splitting works for our method. Section 4 contains numerical examples that show the accuracy of the method for various choices of the numerical parameters. To better judge the quality of our method, we also present an approach that allows us to create a reference solution that is independent of our method.

2. FFT-based method for regularized forces

In this section we concentrate on the case of a single regularized force, which leads to the solution for a general distribution of point forces by the linearity of Stokes equation. Physically, those external point forces could either come from approximating a force distribution along a surface, a curve, or exist on a discrete set of points. Consider the incompressible Stokes equation for periodic flows driven by a regularized force

$$0 = \mu\Delta\mathbf{u} - \nabla p + \mathbf{f}_0\Phi_\varepsilon(\mathbf{x} - \mathbf{x}_n),$$
$$0 = \nabla\cdot\mathbf{u}.$$

We assume that the force $\mathbf{f}_0$ is exerted at $\mathbf{x}_0 \in [0,L]\times[0,L]\times\mathbb{R}$ and is distributed periodically in x and y with period L. Extensions to a rectangular box are straightforward.

Analogously to the singular case, the velocity field can be written as

$$\mu\mathbf{u}(\mathbf{x}) = \big((\mathbf{f}_0\cdot\nabla)\nabla - \mathbf{f}_0\Delta\big)B_{\Phi_\varepsilon}(r),$$

where $r = |\mathbf{x} - \mathbf{x}_0|$ and the Green's function B_{Φ_ε} is the fundamental solution to the biharmonic operator Δ^2, i.e.

$$\Delta G_{\Phi_\varepsilon}(r) = \Phi_\varepsilon(r), \tag{5}$$
$$\Delta B_{\Phi_\varepsilon}(r) = G_{\Phi_\varepsilon}(r). \tag{6}$$

We choose the Gaussian blob function

$$\Phi_\varepsilon(r) = \frac{1}{\varepsilon^3\pi^{\frac{3}{2}}}\left(\frac{5}{2} - \frac{r^2}{\varepsilon^2}\right)\exp\left(-\frac{r^2}{\varepsilon^2}\right), \tag{7}$$

with total integral equal to 1 and which has been used previously by other authors [4,5]. This function is a good choice for two reasons. First, for any smooth function f the difference $(f * \Phi_\varepsilon) - f$, where $*$ stands for the convolution operator, is of order ε^4. In other words, the error introduced by the regularization of the forces decays with forth order as the

regularization parameter ε goes to zero [6]. Second, the form of the blob allows a separation of variables where $\Phi_\varepsilon(r)$ can be written as a sum of two terms of the form $F_1(x,y)F_2(z)$. Consequently, its two-dimensional Fourier transform $\hat{\Phi}_\varepsilon$ can be written as a sum of terms of the form $\hat{F}_1(k,m)F_2(z)$.

For an infinite array of forces distributed periodically in x and y with period L, we incorporate periodicity by using the two-dimensional Fourier transform in x and y, which for an integrable function $g(\mathbf{x})$ is defined as

$$\hat{g}(k,m,z) = \int_{-\infty}^{\infty}\int_{-\infty}^{\infty} g(\mathbf{x}) \exp\big(i(kx+my)2\pi/L\big)\,dx\,dy.$$

We note that when $(k,m)=(0,0)$, the Fourier transform gives a one-dimensional blob in the variable z. When this equation is used to compute the Fourier transform of a function on an $N_g \times N_g$ grid of wave numbers between 0 and $N_g/2$, the values of g on a grid are found using the inverse FFT

$$g(p\Delta x, q\Delta x, z) = \frac{1}{L^2}\sum_{k=0}^{N_g-1}\sum_{m=0}^{N_g-1} \hat{g}(k,m,z)\exp\big(2\pi i(kp+mq)/N_g\big)$$

for $p,q = 0,1,\ldots,N_g-1$ and $\Delta x = L/N_g$.

Taking the two-dimensional Fourier transform of (5) and (6) in the case of one point force $\mathbf{f}_0$ centered at $\mathbf{x}_0=(x_0,y_0,z_0)$, yields the system of ordinary differential equations

$$\hat{G}''_{\Phi_\varepsilon}(\tilde{z}) - c^2\hat{G}_{\Phi_\varepsilon}(\tilde{z}) = \hat{\Phi}_\varepsilon(\tilde{z}), \tag{8}$$

$$\hat{B}''_{\Phi_\varepsilon}(\tilde{z}) - c^2\hat{B}_{\Phi_\varepsilon}(\tilde{z}) = \hat{G}_{\Phi_\varepsilon}(\tilde{z}), \tag{9}$$

where $\tilde{z} = z - z_0$, $c = \frac{2\pi}{L}\sqrt{k^2+m^2}$ where the integers k and m range from 0 to a maximum positive integer. We have omitted the dependence of the functions on (k,m) for notational simplicity and the indicated derivatives are with respect to $\tilde{z}$.

Using the blob function Φ_ε defined in Eq. (7) leads to

$$\hat{\Phi}_\varepsilon(\tilde{z}) = \hat{\delta}^\varepsilon_{x_0y_0}\left[\frac{1}{4\sqrt{\pi}}\left(\frac{6}{\varepsilon}+\varepsilon c^2\right) - \frac{\tilde{z}^2}{\sqrt{\pi}\,\varepsilon^3}\right]\exp\left(-\frac{\tilde{z}^2}{\varepsilon^2}\right)$$

where the factor $\hat{\delta}^\varepsilon_{x_0y_0} = \exp(-\frac{1}{4}\varepsilon^2c^2)\exp(-\frac{2\pi i}{L}(kx_0+my_0))$ contains the dependence on x_0 and y_0.

The goal is to solve Eqs. (8)–(9) exactly for $\hat{B}_{\Phi_\varepsilon}(\tilde{z})$ and determine $\hat{\mathbf{u}}(\tilde{z})$ from the Fourier space analog of (3), which is

$$\begin{aligned}\mu\hat{\mathbf{u}}(\tilde{z}) &= \big((\mathbf{f}_0\cdot\hat{\nabla})\hat{\nabla} - \mathbf{f}_0\hat{\Delta}\big)\hat{B}_{\Phi_\varepsilon}(\tilde{z})\\ &= \begin{pmatrix} \frac{4\pi^2}{L^2}(-f_1k^2 - f_2km)\hat{B}_{\Phi_\varepsilon}(\tilde{z}) + \frac{2\pi i}{L}f_3k\hat{B}'_{\Phi_\varepsilon}(\tilde{z}) - f_1\hat{G}_{\Phi_\varepsilon}(\tilde{z}) \\ \frac{4\pi^2}{L^2}(-f_1km - f_2m^2)\hat{B}_{\Phi_\varepsilon}(\tilde{z}) + \frac{2\pi i}{L}f_3m\hat{B}'_{\Phi_\varepsilon}(\tilde{z}) - f_2\hat{G}_{\Phi_\varepsilon}(\tilde{z}) \\ \frac{4\pi^2}{L^2}f_3(k^2+m^2)\hat{B}_{\Phi_\varepsilon}(\tilde{z}) + \frac{2\pi i}{L}(f_1k+f_2m)\hat{B}'_{\Phi_\varepsilon}(\tilde{z}) \end{pmatrix},\end{aligned} \tag{10}$$

where $\hat{\nabla} = (ik, im, \frac{\partial}{\partial z})$, $\hat{\Delta} = (-k^2-m^2+\frac{\partial^2}{\partial z^2})$, and $\mathbf{f}_0 = (f_1,f_2,f_3)$.

In practice, we solve Eqs. (8)–(9) exactly using a symbolic software package such as Mathematica. Although the wave number pair (k,m) is a parameter in the differential equations, their solutions are all of the same type except when $(k,m)=(0,0)$, or equivalently when $c=0$. We will treat this case separately. For the case $c\neq 0$, it follows that

$$\hat{G}_{\Phi_\varepsilon}(\tilde{z}) = -\frac{\hat{\delta}^\varepsilon_{x_0y_0}}{4c}\exp\left(\frac{\varepsilon^2c^2}{4}\right)\left[\exp(-c\tilde{z})\operatorname{erfc}\left(\frac{c\varepsilon}{2}-\frac{\tilde{z}}{\varepsilon}\right) + \exp(c\tilde{z})\operatorname{erfc}\left(\frac{c\varepsilon}{2}+\frac{\tilde{z}}{\varepsilon}\right)\right] - \frac{\hat{\delta}^\varepsilon_{x_0y_0}\varepsilon}{4\sqrt{\pi}}\exp\left(-\frac{\tilde{z}^2}{\varepsilon^2}\right),$$

and

$$\begin{aligned}\hat{B}_{\Phi_\varepsilon}(\tilde{z}) = {}& \frac{\hat{\delta}^\varepsilon_{x_0y_0}}{8c^3}\exp\left(\frac{c^2\varepsilon^2}{4}\right)\left[(1+c\tilde{z})\exp(-c\tilde{z})\operatorname{erfc}\left(\frac{c\varepsilon}{2}-\frac{\tilde{z}}{\varepsilon}\right) + (1-c\tilde{z})\exp(c\tilde{z})\operatorname{erfc}\left(\frac{c\varepsilon}{2}+\frac{\tilde{z}}{\varepsilon}\right)\right]\\ &+ \frac{\hat{\delta}^\varepsilon_{x_0y_0}\varepsilon}{4\sqrt{\pi}c^2}\exp\left(-\frac{\tilde{z}^2}{\varepsilon^2}\right).\end{aligned}$$

The constants of integrations are chosen so that $\hat{G}_{\Phi_\varepsilon}$ and $\hat{B}_{\Phi_\varepsilon}$ approach 0 as $|z|\to\infty$. Otherwise at least one of the functions $\hat{G}_{\Phi_\varepsilon}$ or $\hat{B}_{\Phi_\varepsilon}$ would grow exponentially in z and this growth would also translate into the velocity. It also follows that

$$\hat{B}'_{\Phi_\varepsilon}(\tilde{z}) = -\frac{\hat{\delta}^\varepsilon_{x_0y_0}}{8c}\exp\left(\frac{c^2\varepsilon^2}{4}\right)\left[\tilde{z}\exp(-c\tilde{z})\operatorname{erfc}\left(\frac{c\varepsilon}{2}-\frac{\tilde{z}}{\varepsilon}\right) + \tilde{z}\exp(c\tilde{z})\operatorname{erfc}\left(\frac{c\varepsilon}{2}+\frac{\tilde{z}}{\varepsilon}\right)\right].$$

It is straightforward to verify that sending $\varepsilon \to 0$ produces

$$\hat{G}(\tilde{z}) = -\frac{\hat{\delta}_{x_0 y_0}}{2c}\exp\left(-c|\tilde{z}|\right) \tag{11}$$

and

$$\hat{B}(\tilde{z}) = \frac{\hat{\delta}_{x_0 y_0}}{4c^2}\left(|\tilde{z}| + \frac{1}{c}\right)\exp\left(-c|\tilde{z}|\right), \tag{12}$$

which solve the singular versions of Eqs. (8)–(9).

For the case $c = 0$, Eq. (10) simplifies to

$$\mu\hat{\mathbf{u}}(\tilde{z}) = \begin{pmatrix} -f_1 \\ -f_2 \\ 0 \end{pmatrix}\hat{G}_{0,\Phi_\varepsilon}(\tilde{z}), \tag{13}$$

and the equation for $\hat{G}_{0,\Phi_\varepsilon}$ simplifies to

$$\hat{G}''_{0,\Phi_\varepsilon}(\tilde{z}) = \left[\frac{3}{2\sqrt{\pi}\varepsilon} - \frac{z^2}{\sqrt{\pi}\varepsilon^3}\right]\exp\left(-\frac{z^2}{\varepsilon^2}\right),$$

with solution

$$\hat{G}_{0,\Phi_\varepsilon}(\tilde{z}) = \frac{1}{4}\left[\frac{\varepsilon}{\sqrt{\pi}}\exp\left(-\frac{\tilde{z}^2}{\varepsilon^2}\right) + 2\tilde{z}\,\mathrm{erf}\left(\frac{\tilde{z}}{\varepsilon}\right)\right].$$

We chose the constants of integration so that sending $\varepsilon \to 0$ yields

$$\hat{G}_0(\tilde{z}) = \frac{|\tilde{z}|}{2}, \tag{14}$$

which solves the singular version of Eq. (8) when $c = 0$. The function $\hat{B}_{0,\Phi_\varepsilon}$ is not needed in this case.

Up to here, all computations can be done analytically. In particular, the divergence of (10) is zero exactly. To complete the evaluation of the velocity field, we fix $\tilde{z}$, evaluate $\hat{\mathbf{u}}(\tilde{z})$ on a grid of wave numbers, and take the inverse FFT. This yields a doubly-periodic velocity field on a two-dimensional grid for the given fixed value of $\tilde{z}$. We emphasize that since all analytic expressions have been found in Fourier space, there is no need to interpolate the forces onto a grid. The only interpolation required is to evaluate the fluid velocity at any point that might not fall onto the grid. Since the velocity is smooth, no special interpolation procedure is needed.

3. Ewald splitting

One approach to solving the doubly-periodic Stokes problem in three dimensions is to begin with Eq. (3), which provides the fluid velocity only due to the N forces exerted in the main domain. To this velocity, we could add the contribution of all the periodic copies of the forces. The result is a double infinite sum that converges slowly in either the physical domain or in the Fourier domain. One way to evaluate the sum efficiently is to separate the velocity formula into a smooth part and a rapidly-decaying part, which can be approximated well and computed fast in the Fourier and physical domains, respectively. The decomposition requires the selection of a splitting parameter ξ that balances the work required to approximate the sums.

Hasimoto [7] was the first to use the splitting into a Fourier space sum and a physical space sum when he computed Stokes flow past periodic arrays of spheres and cylinders. Work by Sierou and Brady [8] and Saintillan et al. [9] uses FFTs to compute the Fourier space sum in an Ewald splitting for triply-periodic domains. They first interpolate the force field onto a regular mesh, take the FFT of the forces, and then compute the velocities using inverse FFTs. Other fast modern numerical methods for triply-periodic arrays of forces include general geometry Ewald-like methods (GGEM) [10] and spectrally accurate methods [11]. Methods dealing with planar periodicity are usually derived from methods solving the triply-periodic problem [2,12]. There the Fourier space sum is evaluated by computing the Fourier integrals exactly. Bleibel [13] develops a formula for doubly-periodic flows in three dimensions for the special case when all interacting particles are within a single plane parallel to the xy-plane.

In the approach presented here, the infinite sum in the Fourier domain has been replaced by an FFT on a grid and the singularity has been removed so that all expressions are smooth. However, the regularization parameter ε is required to be small for numerical accuracy, so that if the grid size Δx is large relative to ε, the FFT may be inaccurate because the grid is not fine enough to capture the smoothness introduced by the right-hand side of Eq. (8). The two obvious remedies, refining the grid or increasing ε, come either at the price of higher computational cost (smaller Δx) or a loss in accuracy (larger ε). Also, if the point forces in Eq. (1) come from approximating a force distribution along a slender body and ε has a physical interpretation such as the thickness of the slender body, ε cannot be chosen freely.

In those cases, we consider the Ewald splitting of the form

$$B_{\Phi_\varepsilon}(r) = \underbrace{B(r)\,\mathrm{erf}\left(\frac{r}{\xi}\right)}_{\text{regular}} + \underbrace{B_{\Phi_\varepsilon}(r) - B(r)\,\mathrm{erf}\left(\frac{r}{\xi}\right)}_{\text{regular and fast decaying}}, \tag{15}$$

where $B(r) = -r/8\pi$ is the Green's function corresponding to the singular problem in (3).

The first term on the right side of Eq. (15) we compute in Fourier space with FFTs as described in Section 2. This procedure requires the splitting parameter ξ to be large enough compared to the grid size in order for the regularization to be resolved on the grid. Note that necessarily $\xi \geqslant \varepsilon$ since otherwise the splitting would not introduce any regularity additional to the one coming from regularizing the forces. In order to compute the velocity field in Fourier space, similar to Section 2 we have to compute the regularized Green's function in Fourier space. The only difference is that in physical space we now start with the Green's function $B_{\Psi_\xi} = B(r)\,\mathrm{erf}(\frac{r}{\xi})$. It turns out that computing the two-dimensional Fourier transform of B_{Ψ_ξ} directly from its definition is not easily done since the term $\mathrm{erf}(r)$ does not allow us to separate the variable z as before. What we do instead is to find twice the Laplacian of B_{Ψ_ξ} to give the corresponding blob function

$$\Psi_\xi(r) = \Delta^2\left(B(r)\,\mathrm{erf}\left(\frac{r}{\xi}\right)\right) = \frac{1}{\xi^3\pi^{\frac{3}{2}}}\left(10 - 11\frac{r^2}{\xi^2} + 2\frac{r^4}{\xi^4}\right)\exp\left(-\frac{r^2}{\xi^2}\right). \tag{16}$$

The blob function Ψ_ξ is quite similar to blob (7) and also has the first three moments equal to zero, which is good for accuracy. The Fourier transform $\Psi_\xi(r)$ is also easy to compute. Once we compute the Fourier transform of Ψ_ξ, we can solve for the corresponding Green's function analytically in Fourier space.

The last two terms on the right side of (15) together we compute directly as a sum of regularized Stokeslets in physical space. We incorporate periodicity by placing copies of forces in the x and y direction. In order to keep computational costs to a minimum, we require the two terms to decay fast, demanding ξ to be as small as possible.

There are two opposing requirements for the splitting parameter ξ. On the one hand we need ξ to be large enough to guarantee enough smoothness for the FFT to be accurate. On the other hand we want ξ to be as small as possible in order to ensure fast decay of the terms in real space. This trade-off is similar to the classical approach where the regular term of the Ewald splitting is computed using infinite series in spectral space. In that approach the splitting parameter ξ is a compromise between a large value, which is desired for the spectral sum to converge fast, and a small value, which is desired for the fast-decaying term to converge fast. Results from [14] indicate that the splitting parameter is best chosen on the order of the period L. In the method presented here, since the regular term is computed with FFTs on a grid, the splitting parameter ξ needs to be only slightly larger than the grid size Δx in order to resolve the blob function on the grid. Therefore, in our method, ξ is typically a small multiple of the grid size. This makes the infinite sum in the last terms in (15) (including the periodic copies of the forces) decay extremely fast. Additionally, the last two terms on the right side of (15) together decay like a Gaussian, which is a consequence of the fact that Φ_ε and Ψ_ξ have second moment zero [15]. The result is that only forces within a cutoff radius of a few ξ need to be considered, as shown in the section of numerical results.

For our method, the splitting in (15) has two advantages over an Ewald splitting of the type used in [2], which has the form

$$B_{\Phi_\varepsilon}(r) = \underbrace{B_{\Phi_\varepsilon}(r)\,\mathrm{erf}\left(\frac{r}{\xi}\right)}_{\text{regular}} + \underbrace{B_{\Phi_\varepsilon}(r)\,\mathrm{erfc}\left(\frac{r}{\xi}\right)}_{\text{regular and fast decaying}}. \tag{17}$$

One reason is that the regular piece in (15) is independent of the blob function Φ_ε and does not need to be recomputed when a different blob is used. In particular, the regular piece is the same even when no blob is used. However, in that case of course the fast-decaying piece would exhibit a singularity. A more practical reason for why we choose the splitting (15) over (17) is that the Fourier transform of the regular piece in (17) is difficult to determine analytically, even when Gaussian blobs are used. This is mainly due to our inability to compute the Fourier transform of $\mathrm{erf}(r)$ in (x, y) only. When we ran into the same problem with splitting (15), we found a remedy in taking two Laplacians. In fact, Eq. (16) eliminates the need to compute the two-dimensional Fourier transform of $\mathrm{erf}(r)$. For splitting (17) even this trick does not work and we are therefore unable to proceed with the FFT-method.

3.1. The formulas in Fourier space

The regular term in (15) can be treated with the methods developed in Section 2, using the expression for velocity in Eq. (10). The only difference is that we use blob (16) instead of (7). To complete the description of this piece, the expressions for $\hat{G}_{\Psi_\xi}$ and $\hat{B}_{\Psi_\xi}$ need to be derived. Replacing the right-hand side in (8) with the Fourier transform of (16) gives

$$\hat{G}''_{\Psi_\xi}(\tilde{z}) - c^2\hat{G}_{\Psi_\xi}(\tilde{z}) = \frac{\hat{\delta}^{\xi}_{x_0y_0}}{8\xi^5\sqrt{\pi}}\left[16\tilde{z}^4 - 56\xi^2\tilde{z}^2 - 8\xi^4\left(-3 + c^2\tilde{z}^2\right) + 6\xi^6c^2 + \xi^8c^4\right]\exp\left(-\frac{\tilde{z}^2}{\xi^2}\right),$$

where again $\tilde{z} = z - z_0$, $c = \frac{2\pi}{L}\sqrt{k^2+m^2}$ and $\hat{\delta}^{\xi}_{x_0y_0} = \exp(-\frac{1}{4}\xi^2c^2)\exp(-\frac{2\pi i}{L}(kx_0+my_0))$. This can be solved exactly to produce for $c \neq 0$

$$\hat{G}_{\Psi_\xi}(\tilde{z}) = -\frac{\hat{\delta}^{\xi}_{x_0y_0}}{4c}\exp\left(\frac{\xi^2c^2}{4}\right)\left[\exp(-c\tilde{z})\operatorname{erfc}\left(\frac{c\xi}{2}-\frac{\tilde{z}}{\xi}\right)+\exp(c\tilde{z})\operatorname{erfc}\left(\frac{c\xi}{2}+\frac{\tilde{z}}{\xi}\right)\right] - \frac{\hat{\delta}^{\xi}_{x_0y_0}}{4\xi\sqrt{\pi}}\left(2\xi^2+\frac{1}{2}\xi^4c^2-2\tilde{z}^2\right)\exp\left(-\frac{\tilde{z}^2}{\xi^2}\right),$$

and subsequently

$$\hat{B}_{\Psi_\xi}(\tilde{z}) = \frac{\hat{\delta}^{\xi}_{x_0y_0}}{8c^3}\exp\left(\frac{c^2\xi^2}{4}\right)\left[(1+c\tilde{z})\exp(-c\tilde{z})\operatorname{erfc}\left(\frac{c\xi}{2}-\frac{\tilde{z}}{\xi}\right)+(1-c\tilde{z})\exp(c\tilde{z})\operatorname{erfc}\left(\frac{c\xi}{2}+\frac{\tilde{z}}{\xi}\right)\right] + \frac{\hat{\delta}^{\xi}_{x_0y_0}\xi}{4\sqrt{\pi}c^2}\left(1+\frac{\xi^2c^2}{2}\right)\exp\left(-\frac{\tilde{z}^2}{\xi^2}\right),$$

as well as

$$\hat{B}'_{\Psi_\xi}(\tilde{z}) = -\frac{\hat{\delta}^{\xi}_{x_0y_0}}{8c}\exp\left(\frac{c^2\xi^2}{4}\right)\left[\tilde{z}\exp(-c\tilde{z})\operatorname{erfc}\left(\frac{c\xi}{2}-\frac{\tilde{z}}{\xi}\right)+\tilde{z}\exp(c\tilde{z})\operatorname{erfc}\left(\frac{c\xi}{2}+\frac{\tilde{z}}{\xi}\right)\right]-\frac{\hat{\delta}^{\xi}_{x_0y_0}\xi}{4\sqrt{\pi}}\tilde{z}\exp\left(-\frac{\tilde{z}^2}{\xi^2}\right).$$

The constants of integration are again chosen so that $\hat{G}_{\Psi_\xi}(\tilde{z})$ and $\hat{B}_{\Psi_\xi}(\tilde{z})$ approach 0 as $|z| \to \infty$ since otherwise the Green's function and the resulting velocity would grow exponentially in z. It is straightforward to verify that taking the limit $\xi \to 0$ produces the singular formulas (11) and (12). If $c = 0$, the solution takes the form

$$\hat{G}_{0,\Psi_\xi}(\tilde{z}) = \frac{\tilde{z}}{2}\operatorname{erf}\left(\frac{\tilde{z}}{\xi}\right)+\frac{\tilde{z}^2}{2\sqrt{\pi}\xi}\exp\left(-\frac{\tilde{z}^2}{\xi^2}\right),$$

where again we chose the constants of integration so that $\hat{G}_{0,\Psi_\xi}$ is a regularized version of (14). The Green's functions can now be readily plugged into (10) and (13), respectively.

3.2. Local sum in physical space

The fast-decaying piece in (15), which can be written as $B_{\Phi_\varepsilon} - B_{\Psi_\xi}$, is treated in infinite space where periodicity is being accounted for by placing periodic copies of the forces in the main domain in the x and y direction. As mentioned before, it suffices to place only copies of forces that fall within a few multiples of ξ from the boundaries of the main domain in each direction because of the Gaussian decay. In detail, solving (5) in spherical coordinates

$$(rG_{\Phi_\varepsilon})'' = r\Phi_\varepsilon(r),$$

where Φ_ε is as in (7), yields the radially symmetric Green's function

$$G_{\Phi_\varepsilon}(r) = -\frac{\operatorname{erf}(\frac{r}{\varepsilon})}{4\pi r}-\frac{\exp(-\frac{r^2}{\varepsilon^2})}{4\varepsilon\pi^{\frac{3}{2}}}.$$

In the limit $\varepsilon \to 0$, this produces $G(r) = -\frac{1}{4\pi r}$ as expected. Similarly, from (4) we obtain

$$B_{\Phi_\varepsilon}(r) = -\frac{r\operatorname{erf}(\frac{r}{\varepsilon})}{8\pi}-\frac{\varepsilon\exp(-\frac{r^2}{\varepsilon^2})}{8\pi^{\frac{3}{2}}} = \frac{-1}{8\pi}\int \operatorname{erf}\left(\frac{r}{\varepsilon}\right)dr, \tag{18}$$

which as $\varepsilon \to 0$ has the limit

$$B(r) = -\frac{r}{8\pi}. \tag{19}$$

Using (18) and (19), the fast-decaying piece in (15) can be represented as

$$B_{\Phi_\varepsilon}(r) - B(r)\operatorname{erf}\left(\frac{r}{\xi}\right) = \frac{r\operatorname{erf}(\frac{r}{\xi}) - r\operatorname{erf}(\frac{r}{\varepsilon})}{8\pi}-\frac{\varepsilon\exp(-\frac{r^2}{\varepsilon^2})}{8\pi^{\frac{3}{2}}}.$$

The velocity field produced by this combination is

$$\left((\mathbf{f}_0\cdot\nabla)\nabla-\mathbf{f}_0\Delta\right)\left(B_{\Phi_\varepsilon}(r)-B(r)\operatorname{erf}\left(\frac{r}{\xi}\right)\right) = \frac{1}{8\pi\mu}\left(\frac{\mathbf{f}_0}{r}C_{\varepsilon,\xi}(r)+\frac{(\mathbf{f}_0\cdot\tilde{\mathbf{x}})\tilde{\mathbf{x}}}{r^3}D_{\varepsilon,\xi}(r)\right), \tag{20}$$

where $\tilde{\mathbf{x}} = \mathbf{x} - \mathbf{x}_0$ and

$$C_{\varepsilon,\xi}(r) = \frac{r}{\sqrt{\pi}}\left[\left(-\frac{6}{\xi} + \frac{4r^2}{\xi^3}\right)\exp\left(-\frac{r^2}{\xi^2}\right) + \frac{2}{\varepsilon}\exp\left(-\frac{r^2}{\varepsilon^2}\right)\right] - \left[\operatorname{erf}\left(\frac{r}{\xi}\right) - \operatorname{erf}\left(\frac{r}{\varepsilon}\right)\right], \tag{21}$$

$$D_{\varepsilon,\xi}(r) = \frac{r}{\sqrt{\pi}}\left[\left(\frac{2}{\xi} - \frac{4r^2}{\xi^3}\right)\exp\left(-\frac{r^2}{\xi^2}\right) - \frac{2}{\varepsilon}\exp\left(-\frac{r^2}{\varepsilon^2}\right)\right] - \left[\operatorname{erf}\left(\frac{r}{\xi}\right) - \operatorname{erf}\left(\frac{r}{\varepsilon}\right)\right]. \tag{22}$$

3.3. Summary of the method

The proposed numerical method using FFTs and Ewald splitting can be summarized as follows. Given N forces $\mathbf{f}_k$ at locations $\mathbf{x}_k$, evaluate the velocity at a point $\mathbf{x} = (x, y, z)$ with the algorithm

1. Evaluate the Fourier transform of the smooth part of the velocity using Eq. (10) for the wavelengths represented on the grid but with B_{Φ_ε} replaced by B_{Ψ_ε} and G_{Φ_ε} replaced by G_{Ψ_ε}. This requires the formulas for G_{Ψ_ε} and B_{Ψ_ε} derived in Section 3.1.
2. Evaluate the smooth part of the velocity via inverse FFT.
3. Add the contribution on the grid from the local velocity using Eqs. (20)–(22). Note that it may be necessary to place a periodic copy of points close to the boundary of the main domain.
4. Interpolate from the grid to the point (x, y, z) if necessary.

A version of the method without the Ewald splitting is:

1. Evaluate the Fourier transform of the entire velocity field using Eq. (10) for the wavelengths represented on the grid. This requires the formulas for G_{Φ_ε} and B_{Φ_ε} derived in Section 2.
2. Evaluate the velocity via inverse FFT.
3. Interpolate from the grid to the point (x, y, z) if necessary.

We note that the algorithm above computes the velocity field on a two-dimensional grid in xy at a height z. The same algorithm must be followed at different values of z where the velocity is needed (see Fig. 1).

4. Numerical results

Consider the case when N regularized forces in random directions are located at random points within the main domain. In order to judge the accuracy of our numerical method developed in the previous two sections, we need a reference solution to compare. We are interested in the error incurred by using FFTs and truncating the sum in physical space, not in the error due to regularizing the forces. In the next section we describe how we compute a reference solution for the regularized force problem that is independent of the method.

4.1. A reference solution

A straightforward way of finding the velocity due to regularized forces is to directly sum the velocity contributions due to the forces and their periodic copies located at $\mathbf{x}_k + \mathbf{n}$, where $\mathbf{n} = (nL, mL, 0)$, i.e.

$$\mu\mathbf{u}(\mathbf{x}) = \sum_{n,m=-\infty}^{\infty}\sum_{k=1}^{N}\big((\mathbf{f}_k\cdot\nabla)\nabla - \mathbf{f}_k\Delta\big)B_{\Phi_\varepsilon}\big(|\mathbf{x}-\mathbf{x}_k-\mathbf{n}|\big).$$

By absorbing the net force into the pressure term of Eq. (1), we can assume a zero net force $\sum_{k=1}^{N}\mathbf{f}_k = 0$ without loss of generality. However, it is inefficient to evaluate the series directly since it converges slowly and only conditionally. Splitting it into a partial sum and a remainder, and using the equivalence of Eqs. (2) and (3) gives

$$\begin{aligned}\mu\mathbf{u}(\mathbf{x}) = &\sum_{n,m=-M}^{M}\sum_{k=1}^{N}\big((\mathbf{f}_k\cdot\nabla)\nabla - \mathbf{f}_k\Delta\big)B_{\Phi_\varepsilon}\big(|\mathbf{x}-\mathbf{x}_k-\mathbf{n}|\big)\\ &+\frac{1}{8\pi}\sum_{\max\{|n|,|m|\}>M}\sum_{k=1}^{N}\frac{\mathbf{f}_k}{|\mathbf{x}-\mathbf{x}_k-\mathbf{n}|} + \frac{[\mathbf{f}_k\cdot(\mathbf{x}-\mathbf{x}_k-\mathbf{n})](\mathbf{x}-\mathbf{x}_k-\mathbf{n})}{|\mathbf{x}-\mathbf{x}_k-\mathbf{n}|^3}\\ &+\sum_{\max\{|n|,|m|\}>M}\sum_{k=1}^{N}\big((\mathbf{f}_k\cdot\nabla)\nabla - \mathbf{f}_k\Delta\big)(B_{\Phi_\varepsilon} - B)\big(|\mathbf{x}-\mathbf{x}_k-\mathbf{n}|\big).\end{aligned} \tag{23}$$

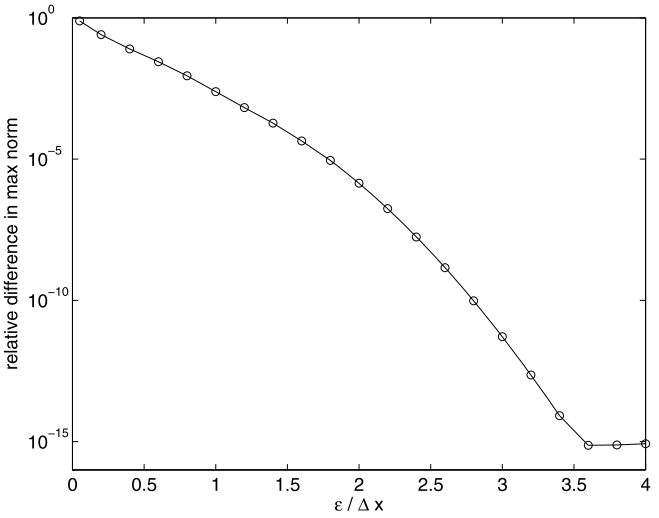

Fig. 2. Relative difference between split ($\xi = 8\Delta x$) and unsplit method on a $64 \times 64 \times 10$ grid (i.e. $\Delta x = \frac{1}{64}$). The flow field was generated by 1000 random forces at random locations inside the cube $[0,1]^3$.

The last term is negligible because for a blob function $\Phi_\varepsilon(r)$ with zero second moment, the velocity due to $B_{\Phi_\varepsilon} - B$ decays like a Gaussian [15]. We ignore this last term from now on. The first term on the right side of (23) containing the partial sums is computed directly using the formula

$$\big((\mathbf{f}_k \cdot \nabla)\nabla - \mathbf{f}_k \Delta\big) B_{\Phi_\varepsilon}(r) = \frac{1}{8\pi}\left(\frac{\mathbf{f}_k}{r} C_\varepsilon(r) + \frac{(\mathbf{f}_k \cdot \tilde{\mathbf{x}})\tilde{\mathbf{x}}}{r^3} D_\varepsilon(r)\right),$$

where $\tilde{\mathbf{x}} = \mathbf{x} - \mathbf{x}_k - \mathbf{n}$, $r = |\tilde{\mathbf{x}}|$, and B_{Φ_ε} as defined in Eq. (18) yields

$$C_\varepsilon(r) = \frac{2r}{\varepsilon\sqrt{\pi}} \exp\left(-\frac{r^2}{\varepsilon^2}\right) + \operatorname{erf}\left(\frac{r}{\varepsilon}\right),$$

$$D_\varepsilon(r) = -\frac{2r}{\varepsilon\sqrt{\pi}} \exp\left(-\frac{r^2}{\varepsilon^2}\right) + \operatorname{erf}\left(\frac{r}{\varepsilon}\right).$$

It remains to estimate the second term on the right side of (23), which represents the error in the truncated sums. It turns out that the leading order terms in this error are linear in $\tilde{\mathbf{x}}$ and can be estimated fairly well. The corresponding formulas are worked out in the appendix. The result is that when $M = 40$, the reference solution is accurate to within 10^{-6}.

4.2. Numerical example

4.2.1. Ewald splitting versus no splitting

We place 1000 random forces with zero net force at random locations inside the cube $[0,1]^3$ and analyze the results produced with and without splitting. We first compute the relative difference between the method implemented without splitting and the method using Ewald splitting for a range of values of ε. For the Ewald splitting implementation, the parameter ξ was fixed to $\xi = 8\Delta x$. This experiment reveals the values of ε for which the Ewald splitting is necessary. The results are in Fig. 2, which shows that the computations agree to within machine precision when $\varepsilon \geqslant 4\Delta x$ or so. Since the splitting parameter ξ plays the role of a regularization parameter, the result also shows that we can choose ξ as small as $\xi = 4\Delta x$ in general, and this provides sufficient smoothness for the FFT computation to be spectrally accurate.

Fig. 2 also shows that when ε is small compared to the grid size Δx, the method without splitting gives solutions that disagree with the Ewald splitting implementation. As ε decreases, the blobs become narrower to the point that they cannot be represented well on the grid, resulting in larger errors. This is verified in Fig. 3 where the two implementations are compared with the reference solution separately. We see that when ε is large enough, both implementations agree. When ε is small relative to Δx, the errors of the method without splitting are large, while the errors of the method with Ewald splitting remain small. We emphasize that the reference solution is only accurate to within 10^{-6} when the series (23) is truncated at $M = 40$. This is why the errors in Fig. 3 saturate around that value. The accuracy of the reference solution is a little better for smaller ε since the remainder term in Eq. (23) is smaller.

4.2.2. Decay of the local sum in an Ewald splitting

In an Ewald splitting, we incorporate periodicity of the local piece in physical space by placing copies of the forces in the main domain in the x and y direction. Since the local piece has fast decay, it contributes to the velocity field only within a

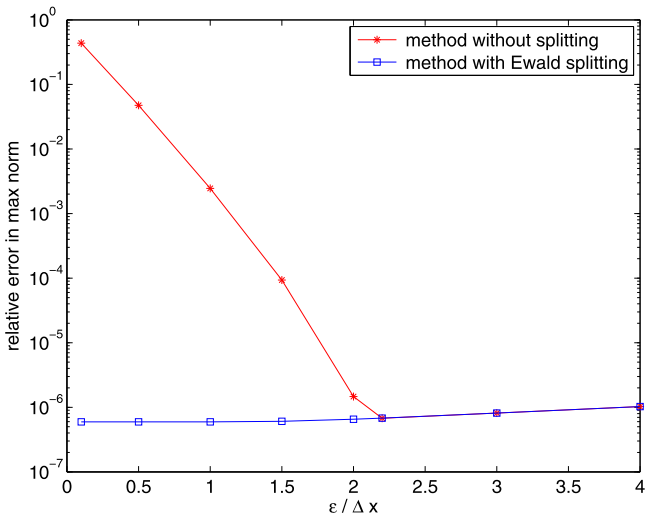

Fig. 3. Relative maximum errors of the velocity field without splitting and with Ewald splitting ($\xi = 4\Delta x$) on a $64 \times 64 \times 10$ grid (i.e. $\Delta x = \frac{1}{64}$). The flow field was generated by 1000 random forces at random locations inside the cube $[0, 1]^3$. For the reference solution we truncated series (23) at $M = 40$ yielding an accuracy of about 10^{-6}.

Table 2
Performance of the split method where the local piece is computed using periodic copies of forces that lie within the cutoff radius of the main domain boundary. The parameters used were $\varepsilon = 4\Delta x$ and $\xi = 6\Delta x$. The results are compared to the reference solution and the solution produced by only using FFTs. For the reference solution we truncated series (23) at $M = 40$ yielding an accuracy of about 10^{-6}.

Cutoff radius	Relative error in max norm	
	$\|\mathbf{u}_{split} - \mathbf{u}_{reference}\|_\infty$	$\|\mathbf{u}_{split} - \mathbf{u}_{unsplit}\|_\infty$
ξ	1.83×10^{-1}	1.83×10^{-1}
2ξ	3.74×10^{-2}	3.74×10^{-2}
4ξ	3.79×10^{-6}	1.32×10^{-6}
6ξ	3.63×10^{-6}	6.99×10^{-15}
8ξ	3.63×10^{-6}	7.88×10^{-16}

certain cutoff radius r_{cutoff}. In order to determine the size of that cutoff radius, we place 1000 random forces with zero net force at random locations inside the cube $[0, 1]^3$. We compute the solution using the Ewald splitting implementation for different values of r_{cutoff} and compare it to the reference solution. The results from Table 2 show that $r_{\text{cutoff}} = 4\xi$ is enough to give us the same accuracy as the reference solution. However, since the accuracy of the reference solution is only about 10^{-6}, we chose the value of the regularization parameter to be $\varepsilon = 4\Delta x$ which is large enough for the FFT method alone (without Ewald splitting) to give accurate results. The last column of Table 2 shows the difference between the methods with and without splitting. We find that the two methods agree to within machine precision already for $r_{\text{cutoff}} = 8\xi$.

4.2.3. Computational cost

We tested the run time of the computations for a range of values $N = 1000$–$32{,}000$ for both implementations of the method, with Ewald splitting and without splitting. The results in Fig. 4 show that the run times of both implementations are linear in N. The method without splitting involves only work to compute the velocity field using FFTs. The method with Ewald splitting requires just as much work to compute the smooth velocity component with FFTs plus additional work to compute the local velocity component, so that the computational cost of the Ewald splitting method will always be larger. From the simulations, it appears that the Ewald splitting implementation takes roughly twice the time of the method without splitting.

We emphasize that the reference solution should not be used as the method of choice when computing periodic Stokes flow. In the FFT setting, it suffices to only consider the N forces in the main domain. If Ewald splitting is used, the computational cost increases by the cost of computing the local piece. Since, in order to achieve machine accuracy, we need to compute the local piece only inside a cutoff radius $r_{\text{cutoff}} = 8\xi$ and we can choose $\xi = 4\Delta x$, usually we can choose a cutoff radius as small as $r_{\text{cutoff}} = 32\Delta x$. In contrast, when computing the reference solution, the number M gives the number of periodic copies of the entire domain in each direction. Hence, for N forces in the main domain, we have to add up $(2M + 1)^2 N$ forces total.

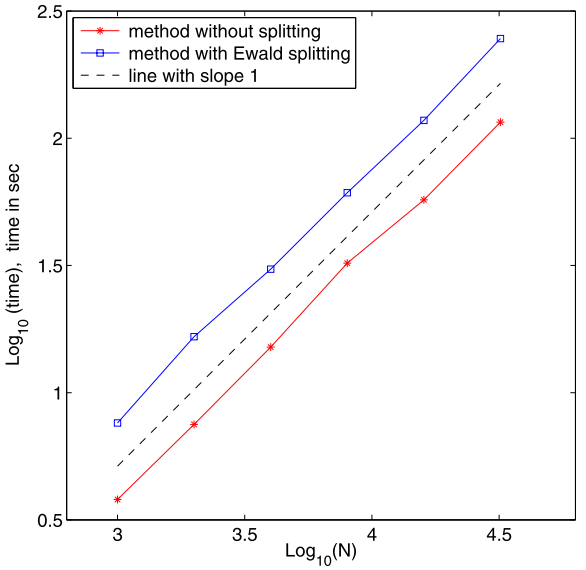

Fig. 4. Run times to compute the velocity field without splitting and with Ewald splitting on a $64 \times 64 \times 1$ grid (i.e. $\Delta x = \frac{1}{64}$). The parameters used were $\varepsilon = 3\Delta x$, $\xi = 4\Delta x$ and $r_{\text{cutoff}} = 8\xi$. The number of point forces in the main domain ranges from $N = 1000$ to $N = 32{,}000$. The dashed line with slope 1 indicates linear scaling in N.

5. Conclusions

We have presented a numerical method for computing doubly periodic Stokes flow driven by regularized point forces in three dimensions. The method is based on computing the smooth component of the flow using FFTs on a regular two-dimensional grid. Ewald splitting is not needed when the forces are regularized with a regularization parameter ε that is large enough compared to the grid size Δx. If Ewald splitting is used in the case where ε is small compared to Δx, there are two advantages. One advantage is that the spectral sum is replaced by an FFT on a grid, which guarantees fast computation. Another advantage is that the FFT allows for the splitting parameter to be chosen as small as $\xi = 4\Delta x$. This makes the sum in physical space converge extremely fast. Numerical experiments have shown that the real space sum needs to be evaluated only within a cutoff radius of $r_{\text{cutoff}} = 8\xi$.

Acknowledgements

The authors thank Tewodros Amdeberhan for contributions to the exact summation in the Appendix and acknowledge support by Louisiana Board of Regents grant LEQSF(2007-12)-ENH-PKSFI-PRS-01.

Appendix A

The goal is to find an approximation for

$$\mu \mathbf{u}_{\text{err}}(\mathbf{x}) = \frac{1}{8\pi} \sum_{\max\{|n|,|m|\}>M} \sum_{k=1}^{N} \frac{\mathbf{f}_k}{|(\mathbf{x}-\mathbf{x}_k)-\mathbf{n}|} + \frac{[\mathbf{f}_k \cdot ((\mathbf{x}-\mathbf{x}_k)-\mathbf{n})]((\mathbf{x}-\mathbf{x}_k)-\mathbf{n})}{|(\mathbf{x}-\mathbf{x}_k)-\mathbf{n}|^3},$$

where $\mathbf{n} = (nL, mL, 0)$. Using the notation $\hat{n} = \frac{\mathbf{n}}{|\mathbf{n}|}$, we find

$$\big|(\mathbf{x}-\mathbf{x}_k)-\mathbf{n}\big|^2 = \big[(\mathbf{x}-\mathbf{x}_k)-\mathbf{n}\big] \cdot \big[(\mathbf{x}-\mathbf{x}_k)-\mathbf{n}\big] = \underbrace{|\mathbf{x}-\mathbf{x}_k|^2}_{=:D_0} \underbrace{- 2\big[(\mathbf{x}-\mathbf{x}_k)\cdot\hat{n}\big]}_{=:D_1} |\mathbf{n}| + |\mathbf{n}|^2,$$

and also

$$\begin{aligned}\big[\mathbf{f}_k \cdot \big((\mathbf{x}-\mathbf{x}_k)-\mathbf{n}\big)\big]\big((\mathbf{x}-\mathbf{x}_k)-\mathbf{n}\big) &= \big[\mathbf{f}_k \cdot (\mathbf{x}-\mathbf{x}_k) - \mathbf{f}_k \cdot \mathbf{n}\big]\big[(\mathbf{x}-\mathbf{x}_k)-\mathbf{n}\big] \\ &= \underbrace{\big[\mathbf{f}_k \cdot (\mathbf{x}-\mathbf{x}_k)\big](\mathbf{x}-\mathbf{x}_k)}_{=:B_0} \underbrace{- \big(\big[\mathbf{f}_k \cdot (\mathbf{x}-\mathbf{x}_k)\big]\hat{n} + [\mathbf{f}_k \cdot \hat{n}](\mathbf{x}-\mathbf{x}_k)\big)}_{=:B_1} |\mathbf{n}| \\ &\quad + \underbrace{[\mathbf{f}_k \cdot \hat{n}]\hat{n}}_{=:B_2} |\mathbf{n}|^2.\end{aligned}$$

Further defining $A_0 := \mathbf{f}_k$, an asymptotic expansion of the Stokeslet in powers of $s := |\mathbf{n}|$ at ∞ is given by

$$\begin{aligned}
&\frac{1}{8\pi}\left(\frac{A_0}{(D_0+D_1 s+s^2)^{\frac{1}{2}}}+\frac{B_0+B_1 s+B_2 s^2}{(D_0+D_1 s+s^2)^{\frac{3}{2}}}\right)\\
&=\frac{A_0+B_2}{8\pi s}+\frac{2B_1-A_0D_1-3B_2D_1}{16\pi s^2}+\frac{8B_0-4A_0D_0-12B_2D_0-12B_1D_1+3A_0D_1^2+15B_2D1^2}{64\pi s^3}\\
&\quad+\frac{-24B_1D_0-24B_0D_1+12A_0D_0D_1+60B_2D_0D_1+30B_1E_1^2-5A_0E_1^3-35B_2E_1^3}{128\pi s^4}+\mathcal{O}\left(\frac{1}{s^5}\right).
\end{aligned}$$

When we sum over k, m and n, a lot of these terms cancel. In detail, the $\frac{1}{s}$ term cancels because of the zero net force. Further, note that the subindices of A, B and D represent the order of $\hat{n}$. In particular, the coefficients of $\frac{1}{s^2}$ and $\frac{1}{s^4}$ are odd in $\hat{n}$. So when we sum over positive and negative m as well as positive and negative n symmetrically, these terms cancel as well. What is left is

$$\mathbf{u}_{\mathrm{err}}(\mathbf{x})=\frac{1}{8\pi}\sum_{\max\{|n|,|m|\}>M}\sum_{k=1}^{N}\frac{8B_0-4A_0D_0-12B_2D_0-12B_1D_1+3A_0D_1^2+15B_2D1^2}{8s^3}+\mathcal{O}\left(\frac{1}{s^5}\right).$$

The coefficient of $\frac{1}{s^3}$ is quadratic in $\mathbf{x}$. However, ultimately the quadratic terms in $\mathbf{x}$ cancel because of the zero net force. Hence, $\mathbf{u}_{\mathrm{err}}$ is linear in $\mathbf{x}$ up to $\mathcal{O}(\frac{1}{s^5})$. We find

$$\mathbf{u}_{\mathrm{err}}(\mathbf{x})\approx\begin{pmatrix} S_1^{M^+} & S_2^{M^+} & S_3^{M^+} & S_4^{M^+}\end{pmatrix}\begin{pmatrix}\mathbf{a}_{11} & \mathbf{a}_{1x} & \mathbf{a}_{1y} & \mathbf{a}_{1z}\\ \mathbf{a}_{21} & \mathbf{a}_{2x} & \mathbf{a}_{2y} & \mathbf{a}_{2z}\\ \mathbf{a}_{31} & \mathbf{a}_{3x} & \mathbf{a}_{3y} & \mathbf{a}_{3z}\\ \mathbf{a}_{41} & \mathbf{a}_{4x} & \mathbf{a}_{4y} & \mathbf{a}_{4z}\end{pmatrix}\begin{pmatrix}1\\ x\\ y\\ z\end{pmatrix},$$

where

$$\mathbf{a}_{11}=\begin{pmatrix}x_k(f_1x_k+f_2y_k+f_3z_k)-\frac{1}{2}f_1(x_k^2+y_k^2+z_k^2)\\ y_k(f_1x_k+f_2y_k+f_3z_k)-\frac{1}{2}f_2(x_k^2+y_k^2+z_k^2)\\ z_k(f_1x_k+f_2y_k+f_3z_k)-\frac{1}{2}f_3(x_k^2+y_k^2+z_k^2)\end{pmatrix},$$

$$\mathbf{a}_{21}=\begin{pmatrix}-6f_1x_k^2-6f_2x_ky_k-3f_3x_kz_k-\frac{3}{2}f_1z_k^2\\ -6f_1x_ky_k-6f_2y_k^2-3f_3y_kz_k-\frac{3}{2}f_2z_k^2\\ \frac{3}{2}f_3x_k^2+\frac{3}{2}f_3y_k^2-3f_1x_kz_k-3f_2y_kz_k\end{pmatrix},$$

$$\mathbf{a}_{31}=\begin{pmatrix}\frac{15}{2}f_1x_k^2\\ \frac{15}{2}f_2y_k^2\\ 0\end{pmatrix},\qquad \mathbf{a}_{41}=\begin{pmatrix}15f_2x_ky_k+\frac{15}{2}f_1y_k^2\\ 15f_1x_ky_k+\frac{15}{2}f_2x_k^2\\ 0\end{pmatrix},$$

$$\mathbf{a}_{1x}=\begin{pmatrix}-f_1x_k-f_2y_k-f_3z_k\\ f_2x_k-f_1y_k\\ f_3x_k-f_1z_k\end{pmatrix},\qquad \mathbf{a}_{2x}=\begin{pmatrix}12f_1x_k+6f_2y_k+3f_3z_k\\ 6f_1y_k\\ -3f_3x_k+3f_1z_k\end{pmatrix},$$

$$\mathbf{a}_{3x}=\begin{pmatrix}-15f_1x_k\\ 0\\ 0\end{pmatrix},\qquad \mathbf{a}_{4x}=\begin{pmatrix}-15f_2y_k\\ -15f_2x_k-15f_1y_k\\ 0\end{pmatrix},$$

$$\mathbf{a}_{1y}=\begin{pmatrix}-f_2x_k+f_1y_k\\ -f_1x_k-f_2y_k-f_3z_k\\ f_3y_k-f_2z_k\end{pmatrix},\qquad \mathbf{a}_{2y}=\begin{pmatrix}6f_2x_k\\ 6f_1x_k+12f_2y_k+3f_3z_k\\ -3f_3y_k+3f_2z_k\end{pmatrix},$$

$$\mathbf{a}_{3y}=\begin{pmatrix}0\\ -15f_2y_k\\ 0\end{pmatrix},\qquad \mathbf{a}_{4y}=\begin{pmatrix}-15f_2x_k-15f_1y_k\\ -15f_1x_k\\ 0\end{pmatrix},$$

$$\mathbf{a}_{1z}=\begin{pmatrix}-f_3x_k+f_1z_k\\ -f_3y_k+f_2z_k\\ -f_1x_k-f_2y_k-f_3z_k\end{pmatrix},\qquad \mathbf{a}_{2z}=\begin{pmatrix}3f_3x_k+3f_1z_k\\ 3f_3y_k+3f_2z_k\\ 3f_1x_k+3f_2y_k\end{pmatrix},$$

$$\mathbf{a}_{3z}=\begin{pmatrix}0\\ 0\\ 0\end{pmatrix},\qquad \mathbf{a}_{4z}=\begin{pmatrix}0\\ 0\\ 0\end{pmatrix},$$

where $\mathbf{f} = (f_1, f_2, f_3)$, $\mathbf{x} = (x, y, z)$, $\mathbf{x}_k = (x_k, y_k, z_k)$, and

$$S_1^{M+} = \frac{1}{8\pi L^3} \cdot \sum_{\max\{|n|,|m|\}>M} \frac{1}{(n^2+m^2)^{\frac{3}{2}}},$$

$$S_2^{M+} = \frac{1}{8\pi L^3} \cdot \sum_{\max\{|n|,|m|\}>M} \frac{n^2}{(n^2+m^2)^{\frac{5}{2}}},$$

$$S_3^{M+} = \frac{1}{8\pi L^3} \cdot \sum_{\max\{|n|,|m|\}>M} \frac{n^4}{(n^2+m^2)^{\frac{7}{2}}},$$

$$S_4^{M+} = \frac{1}{8\pi L^3} \cdot \sum_{\max\{|n|,|m|\}>M} \frac{n^2m^2}{(n^2+m^2)^{\frac{7}{2}}}.$$

In order to compute the sums we write, for instance in the case of S_1^{M+},

$$\sum_{\max\{|n|,|m|\}>M} \frac{1}{(n^2+m^2)^{\frac{3}{2}}} = \sum_{\substack{(n,m)\neq(0,0)\\ n,m=-\infty}}^{\infty} \frac{1}{(n^2+m^2)^{\frac{3}{2}}} - \sum_{\substack{(n,m)\neq(0,0)\\ n,m=-M}}^{M} \frac{1}{(n^2+m^2)^{\frac{3}{2}}}.$$

On the right-hand side, the partial sum can be computed during execution depending on what M is chosen while the infinite series is independent of M and can be computed beforehand. The same argument applies to the three other sums. We find

$$S_1 := \sum_{(n,m)\neq(0,0)} \frac{1}{(n^2+m^2)^{\frac{3}{2}}} = 9.033621683100950\ldots,$$

$$S_2 := \sum_{(n,m)\neq(0,0)} \frac{n^2}{(n^2+m^2)^{\frac{5}{2}}} = 4.516810841550475\ldots,$$

$$S_3 := \sum_{(n,m)\neq(0,0)} \frac{n^4}{(n^2+m^2)^{\frac{7}{2}}} = 3.745708094289508\ldots,$$

$$S_4 := \sum_{(n,m)\neq(0,0)} \frac{n^2m^2}{(n^2+m^2)^{\frac{7}{2}}} = 0.771102747260967\ldots.$$

These numerical estimates are hard to find through direct evaluation because of the slow convergence. We will show how to find good estimates for S_1 and S_4, which by means of the relationship

$$S_1 = 2S_2 = 2(S_3 + S_4),$$

also give good estimates for the remaining two sums. S_1 is know to be exactly equal to $S_1 = 4\zeta(\frac{3}{2})\beta(\frac{3}{2})$, where $\zeta(t) = \sum_{k=1}^{\infty} \frac{1}{k^t}$ is the classical Riemann zeta function and $\beta(t) = \sum_{k=0}^{\infty} \frac{(-1)^k}{(2k+1)^t}$ is the Dirichlet beta function. S_4 is rewritten as an infinite sum of Bessel functions of the second kind, which have exponential decay. Therefore the series is easy to evaluate numerically.

Lemma. *It holds true that*

$$S_4 = \frac{4\pi^2}{45} - \frac{32\pi^3}{15} \sum_{m,n=1}^{\infty} mn^3\big(K_1(2\pi mn) + K_3(2\pi mn)\big) + \frac{32\pi^2}{5} \sum_{m,n=1}^{\infty} n^2 K_2(2\pi mn),$$

where $K_\nu(t)$ is the modified Bessel function of the second kind of degree ν.

Proof. It follows from Hankel's generalization of the Lipschitz integral that [16, Ch. 13.2]

$$\frac{2^\nu \Gamma(\nu+\frac{1}{2}) m^\nu}{\sqrt{\pi}(n^2+m^2)^{(\nu+\frac{1}{2})}} = \int_0^\infty e^{-|n|t} J_\nu(mt) t^\nu \, dt,$$

where $J_\nu(t)$ is the Bessel function of the first kind of order ν. Setting $\nu = 2$ and using $\Gamma(\frac{5}{2}) = \frac{3\sqrt{\pi}}{4}$, gives

$$\frac{m^2}{(n^2+m^2)^{\frac{5}{2}}} = \frac{1}{3}\int_0^\infty e^{-|n|t} J_2(mt) t^2\, dt.$$

Writing the equation as

$$\frac{m^2}{(n^2x+m^2)^{\frac{5}{2}}} = \frac{1}{3}\int_0^\infty e^{-|n|\sqrt{x}t} J_2(mt) t^2\, dt,$$

and differentiating with respect to x, gives

$$-\frac{5}{2}\cdot\frac{m^2n^2x}{(n^2x+m^2)^{\frac{7}{2}}} = \frac{1}{3}\int_0^\infty -\frac{|n|t}{2\sqrt{x}} e^{-|n|\sqrt{x}t} J_2(mt) t^2\, dt.$$

Note that we can switch the order of differentiation and integration by the Lebesgue dominated convergence theorem for $n \neq 0$. Also note that since the new formula trivially holds for $n = 0$, in fact it holds for all real n. Setting $x = 1$ produces

$$\frac{m^2n^2}{(n^2+m^2)^{\frac{7}{2}}} = \frac{1}{15}\int_0^\infty |n| e^{-|n|t} J_2(mt) t^3\, dt.$$

The rest of the proof is analogous to [17,18]. It follows that

$$\begin{aligned} S_4 &= 2\sum_{m=1}^\infty \sum_{n=-\infty}^\infty \frac{m^2n^2}{(n^2+m^2)^{\frac{7}{2}}} \\ &= \frac{2}{15}\sum_{m=1}^\infty \int_0^\infty \sum_{n=-\infty}^\infty |n| e^{-|n|t} J_2(mt) t^3\, dt = \frac{4}{15}\sum_{m=1}^\infty \int_0^\infty J_2(mt)\frac{t^3e^t}{(-1+e^t)^2}\, dt. \end{aligned}$$

Computing the residues of the function $g(z) = H_2^{(1)}(mz)\frac{z^3e^z}{(-1+e^z)^2}$ in the upper half plane [17], where $H_\nu^{(1)}$ is the first Hankel function of degree ν, completes the proof. □

References

[1] P. Lenz, A. Ryskin, Collective effects in ciliar arrays, Phys. Biol. 3 (2006) 285–294.
[2] C. Pozrikidis, Computation of periodic Green's functions of Stokes flow, J. Eng. Math. 30 (1996) 79–96.
[3] R. Cortez, The method of regularized stokeslets, SIAM J. Sci. Comput. 23 (4) (2001) 1204–1225.
[4] J.P. Hernández-Ortiz, J.J. de Pablo, M.D. Graham, Fast computation of many-particle hydrodynamic and electrostatic interactions in a confined geometry, Phys. Rev. Lett. 98 (2007) 140602, http://dx.doi.org/10.1103/PhysRevLett.98.140602.
[5] A. Kumar, M.D. Graham, Accelerated boundary integral method for multiphase flow in non-periodic geometries, J. Comput. Phys. 231 (20) (2012) 6682–6713, http://dx.doi.org/10.1016/j.jcp.2012.05.035.
[6] R. Cortez, L. Fauci, A. Medovikov, The method of regularized Stokeslets in three dimensions: Analysis, validation, and application to helical swimming, Phys. Fluids 17 (3) (2005) 031504.
[7] H. Hasimoto, On the periodic fundamental solutions of the Stokes equations and their application to viscous flow past a cubic array of spheres, J. Fluid Mech. 5 (1959) 317–328.
[8] A. Sierou, J.F. Brady, Accelerated stokesian dynamics simulations, J. Fluid Mech. 448 (2001) 115–146, http://dx.doi.org/10.1017/S0022112001005912.
[9] D. Saintillan, E. Darve, E.S.G. Shaqfeh, A smooth particle-mesh Ewald algorithm for Stokes suspension simulations: The sedimentation of fibers, Phys. Fluids 17 (3) (2005) 033301, http://dx.doi.org/10.1063/1.1862262, http://link.aip.org/link/?PHF/17/033301/1.
[10] J.P. Hernàndez-Ortiz, J.J. de Pablo, M.D. Graham, Fast computation of many-particle hydrodynamic and electrostatic interactions in a confined geometry, Phys. Rev. Lett. 98 (2007) 140602, 4 pp.
[11] D. Lindbo, A.-K. Tornberg, Spectrally accurate fast summation for periodic Stokes potentials, J. Comput. Phys. 229 (2010) 8994–9010.
[12] D. Lindbo, A.-K. Tornberg, Fast and spectrally accurate summation of 2-periodic Stokes potentials, arXiv:1111.1815v1 [physics.flu-dyn].
[13] J. Bleibel, Ewald sum for hydrodynamic interactions with periodicity in two dimensions, J. Phys. A, Math. Theor. 45 (22) (2012) 225002, http://stacks.iop.org/1751-8121/45/i=22/a=225002.
[14] C.W.J. Beenakker, Ewald sum of the Rothe–Prager tensor, J. Chem. Phys. 85 (1986) 1581–1582.
[15] K. Leiderman, E.L. Bouzarth, R. Cortez, A.T. Layton, A regularization method for the numerical solution of periodic Stokes flow, J. Comput. Phys. 236 (2013) 187–202.
[16] G.N. Watson, A Treatise on the Theory of Bessel Functions, 2nd edition, Cambridge University Press, 1966.
[17] N. Liron, S. Mochon, Stokes flow for a stokeslet between two parallel flat plates, J. Eng. Math. 10 (4) (1976) 287–303.
[18] N. Liron, Stokes flow due to infinite arrays of stokeslets in three dimensions, J. Eng. Math. 30 (1995) 267–297.